Supplementary Material

Supplementary Methods

iTARQ-based proteomics analysis

The left ventricular tissues from tamoxifen or diluent injected MCM/LRP6$^{fl/fl}$ were analyzed to identify differentiated protein by iTARQ-based proteomics technique as described in previous study [1]. In brief, total protein was concentrated and extracted from left ventricular tissues at day 1 after tamoxifen or diluent injected MCM/LRP6$^{fl/fl}$. The protein concentration was determined with Bradford assay kit (Bio-Rad). Equal amounts of protein were labeled with iTARQ reagent. Control was labeled with 113 and 114; MO was labeled with 115 and 116.Each labeled sample includes mixture of two protein samples from two mice of same group. The labeled samples were combined and dried in vacuo for LC-MS/MS analysis. To identify and quantitate protein, LC-MS/MS data were analyzed with the proteinPilot 2.0 software (Applied Biosytems). The iTRAQ ratio ≥1.2 or ≤0.83 was considered as up or down regulation [2, 3], respectively.

Mitochondrial isolation and purification.

Mitochondria were isolated from adult mouse heart tissues by mitochondrial isolation kit (Beyotime) according to manual instruction. Isolated mitochondria were resuspended in ethylene glycol tetraacetic acid (EGTA)-free homogenization buffer to further analysis. Mitochondria were kept on ice and conducted experiments within 4 h.

The crude mitochondrial pellet was re-suspended in 19% percoll with isolation buffer [4], and layered slowly on two layers in 30% and 60% percoll (v/v). After centrifugation for 15min at 10,000g, mitochondrial pellet were corrected and wash for 3 times with isolation buffer. The final purified mitochondria were stored at -80^{0}C for further analysis.

Thoracic aortic constriction (TAC) in Mice.

Tamoxifen (30mg/kg i.p.) or diluent was injected to 8-10-week MCM-LRP6$^{fl/+}$ mice for 3 consecutive days, a week later, pressure overload was induced by thoracic aorta constriction (TAC) in these mice as in our previous study [5]. After anaesthetized with ketamine (25mg/kg i.p.), mice were subjected to TAC operation by ligating the aorta with 7-0 nylon suture against a blunted 27-gauge needle which was pulled later. All of the animal experiments were approved by the Animal Care and Use Committee of Fudan University and performed according to the Guidelines for the Care and Use of Laboratory Animals (published by the National Academy Press (NIH Publication No. 85-23, revised 1996).

Mitochondrial membrane potential assay.

Mitochondrial membrane potential was measured by a mitochondrial membrane potential assay kit (Beyotime) with 5,5',6,6'- tetrachloro-1,1',3,3'-tetraethylbenzimidazolocarbocyanine iodide (JC-1), a cell-penetrating lipophilic cationic fluorochrome that accumulates in energized mitochondria. At low ΔΨm (low mitochondrial membrane potential), JC-1 is predominantly a monomer that

yields green fluorescence. At high ΔΨm, the dye aggregates yielding a red to orange colored emission. When mitochondrial membrane becomes depolarized, a decrease of red to green fluorescence ratio will be detected by Fluorence microplate reader. CCCP (10μM) was used to induce mitochondrial depolarization as positive control. Mitochondrial depolarization of ΔΨm was expressed as green to red fluorescence ratio as in previous study [6].

Mitochondrial swelling assay.

The mitochondrial swelling assay was performed to determine opening of MPT pores as described [7]. In brief, isolated cardiac mitochondria were suspended in a swelling buffer (120 mM KCl, 10 mM Tris HCl (PH 7.6),20 mM MOPS, and 5 mM KH_2PO_4) to a final mitochondrial protein concentration of 0.25mg/ml. The mitochondrial suspensions were incubated with 50μM CaCl2 (calcium chloride) in a final volume of 200μl in a 96-well plate for 30 min. Absorbance was read at 520 nm (A520), and the reduction at A520 was measured.

ATP production assay.

Cardiac ATP level was determined by an ATP assay kit (Beyotime) as in previous study[8]. 20mg of heart tissue was homogenized in ice-cold ATP lysis buffer. The homogenate was centrifuged at 12000g for 10 min at 4 °C to collect the supernatant. 100 μl ATP detection working solution was added to a black 96-well plate. After 5 minutes, the supernatant was added to the wells and the luminescence was measured quickly. The measurement was normalized by the protein concentration of each well.

Mitochondrial complex activity assay.

Mitochondrial complex activities were examined by MitoCheck Complex I, II/III (Cayman Chemical Company, USA) and IV (Sigma USA) Activity Assay Kit according to manual described as previous study [9]. In brief, complex I activity and complex II/III activity were assayed by monitoring the rotenone-sensitive ubiquinone-1 (Q1)-stimulated NADH oxidation and the rate of reduced cytochrome c formation respectively. Complex IV activity was analyzed by evaluating ferrocytochrome c oxidation. The complex activities were normalized by mitochondrial weight.

Transmission electron microscopy

Freshly isolated heart tissue was fixed in fresh 2.5% glutaraldehyde for 2h at 4°C, washed in phosphate buffer, and post-fixed in 1% osmium tetroxide (OsO_4) solution for another 2 h. The hearts were dehydrated in an ethanol gradient and then embedded in epoxy resin 618 (Shanghai Resin Factory, Shanghai,China). The heart tissues were sliced into 70-nm thick sections with a Reichert Ultracut E ultramicrotome (Leica, Heidelberg, Germany), staining with uranyl acetate and lead citrate for 1 h. Examination was carried out under a Philips CM120 electron microscope (RoyalDutch Philips Electronics Ltd, Amsterdam, the Netherlands) at 60 kV.

Oil red O staining

Heart sections were stained Oil red O as described in recent study [10]. The frozen heart sections were fixed by acetone. After wash with PBS, the slides

were stained with Oil red O staining. The background was cleared using 60% isopropanol. The lipid was stained with red and observed under microscope.

GC-FID/MS analysis of fatty acid composition in heart tissue.

Fatty acid composition in heart tissue was measured in the methylated forms as previous study with some modifications [11]. About 6 mg heart tissue was homogenized with 700μL of methanol using Tissue Lyser (QIAGEN TissueLyser II, Germany) at 20 Hz for 90 s three times (one-minute breaks between three homogenizations) followed by 10-min intermittent sonication (30 s sonication and 30 s break) in an ice bath. After methylated, fatty acids were analyzed by 7890B Gas Chromatograph (GC) 5977A Mass Selective Detector (MSD) (Agilent Technologies, USA) equipped with a flame ionization detector (FID) and a mass spectrometer with an electron impact (EI) ion source. An Agilent DB-225 capillary GC column (10 m, 0.1 mm ID, 0.1 μm film thickness) was used with sample injection volume of 1 μL and a splitter (1:30). The injection port and detector temperatures were set at 230 °C. The column temperature was programmed with 55 °C for 1 min and then increased to 205 °C with a rate of 30 °C per min. Colum temperature was kept at 205 °C for following 3 min and increased to 230 °C at 5 °C per min. For identification, these methylated fatty acids were compared with a chromatogram from a mixture of 37 known standards and then confirmed with their mass spectral data. Each fatty acid was quantified with the FID data by comparing its signal integrals with peak integrals of internal standards. The data were expressed

as μmol of fatty acids per gram of tissue. The molar percentages were calculated from the above data for unsaturated fatty acids (UFA), saturated fatty acids (SFA), polyunsaturated fatty acids (PUFA) and monounsaturated fatty acids (MUFA), respectively.

Real-time PCR analysis

We performed quantitative PCR by Bio-Rad iQ5 (Bio-Rad, Philadelphia, PA, USA) using SYBR green. The primers we used were provided in Table S2. We normalized the amount of mtDNA to that of nDNA or mRNAs of target genes to GAPDH and then calculated the ratio of mtDNA content or mRNA in LRP6 deletion heart to that in control littermates.

Table S1. All the primary antibodies used in the Western blot analysis.

Antibody	Company	Catalog#	-Size（kDa）	2°
LRP6(C47E12)Rabbit mAb	Cell Signaling Technology, BOSTON	3395	180	Rabbit
LRP6 (C5C7) Rabbit mAb	Cell Signaling Technology, BOSTON	2560	180	Rabbit
LRP5(D80F2)Rabbit mAb	Cell Signaling Technology,BOSTON	5731	200	Rabbit
Phospho-DRP1(Ser616) Antibody	Cell Signaling Technology, BOSTON	3455	78-82	Rabbit
DRP1(D6C7) Rabbit mAb	Cell Signaling Technology, BOSTON	8570	78-82	Rabbit
AMPKα Antibody	Cell Signaling Technology, BOSTON	2532	62	Rabbit
Phospho-AMPKα (Thr172) (40H9) Rabbit mAb	Cell Signaling Technology, BOSTON	2535	62	Rabbit
mTOR(7C10) Rabbit mAb	Cell Signaling Technology, BOSTON	2983	289	Rabbit

Phospho-mTOR (Ser2448) Antibody	Cell Signaling Technology BOSTON	2971	289	Rabbit
β-Catenin (6B3) Rabbit mAb	Cell Signaling Technology, BOSTON	9582	92	Rabbit
VDAC1 Antibody	Cell Signaling Technology, BOSTON	4866	32	Rabbit
Phospho-p44/42MAPK (Erk1/2) (Thr202/Tyr204) Antibody	Cell Signaling Technology,BOSTON	9101	42, 44	Rabbit
p44/42 MAPK (Erk1/2) (137F5) Rabbit mAb	Cell Signaling Technology, BOSTON	4695	42,44	Rabbit
LRP5(D80F2)Rabbit mAb	Cell Signaling Technology,BOSTON	5731	200	Rabbit
Rabbit anti-PINK1 polyclonal Antibody	Proteintech Chicago	23274-1-AP	65,45	Rabbit
Rabbit anti P62/SQSTM1 polyclonal Antibody	Proteintech Chicago	18420-1-AP	62	Rabbit
Rabbit anti- Histone-H3 polyclonal Antibody	Proteintech Chicago	17168-1-AP	15-17	Rabbit
HRP-conjugated Mouse anti GAPDH monoclonal Antibody	Proteintech Chicago	HRP-60004	36	Mouse
PAKIN Antibody	Abcam Cambridge	ab15954	51.6	Rabbit
FOUND1 Antibody	Abcam, Cambridge	ab74834	17	Rabbit
LC3B Antibody	Abcam, Cambridge	ab63817	15	Rabbit
LC3B Antibody	Cell Signaling Technology, BOSTON	2775	14,16	Rabbit
PPARalpha antibody	Abcam, Cambridge	ab24509	52	Rabbit
PGC1alpha antibody	Abcam, Cambridge	ab54481	92	Rabbit
PPARdelta antibody	Abcam, Cambridge	Ab23673	50	Rabbit
Tom22 antibody	Santa Cruz Biotechnology Inc Delaware Avenue	Sc-14896	22	Rabbit
TFEB antibody	Abcam, Cambridge	Ab2636	53	Rabbit

Active β-catenin (clone 8E7) monoclonal antibody	Millipore upstate	05665	92	Mouse

Table S2. All the primers in Real-time PCR analysis.

Gene name	Sequence 5'-3'	
GAPDH	Forward	ACCACAGTCCATGCCATCAC
	Reverse	TCCACCACCCTGTTGCTGTA
Axin2	Forward	AGCCGCCATAGTC
	Reverse	GGTCCTCTTCATAGC
Lef-1	Forward	GTCCCTTTCTCCACCCATC
	Reverse	AAGTGCTCGTCGCTGTAG
Tcf7l2	Forward	AAACAGCTCTCCGATTCCG
	Reverse	CTCGGAAACTTTCGGAGCGA
Fas	Forward	GATCCTGGAACGAGAACAC
	Reverse	AGACTGTGGAACACGGTGGT
Scd-1	Forward	CGAGGGTTGGTTGTTGATCTGT
	Reverse	ATAGCACTGTTGGCCCTGGA
Acc1	Forward	GACGTTCGCCATAACCAAGT
	Reverse	CTGTTTAGCGTGGGGATGTT
Pparγ	Forward	AGCATGGTGCCTTCGCTGATGC
	Reverse	AAGTTGGTGGGCCAGAATGGCA
H19	Forward	GTACCCACCTGTCGTCC
	Reverse	GTCCACGAGACCAATGACTG
mt-Nd1	Forward	AATCGCCATAGCCTTCCTAACAT
	Reverse	GGCGTCTGCAAATGGTTGTAA
mt-Cytb	Forward	TTCTGAGGTGCCACAGTTATT
	Reverse	GAAGGAAAGGTATT AGGGCTAAA
mt-Cox1	Forward	CCCA ATCTCTACCAGCATC
	Reverse	GGCTCATAGTATAGCTGGAG

Table S3. Basic characteristic of human cardiac samples with dilated cardiomyopathy (DCM) or not (Control).

	Control			DCM		
Number	HS01	HS03	HS17	ZS13167553	ZS14253892	ZS13274801
Age	42	47	49	41	40	47
Sex	Male	Male	Male	Male	Male	Male
EF	70%	63%	62%	25%	32%	20%

Table S4. Basic characteristic of MCM and MCM/LRP6$^{fl/fl}$ mice before tamoxifen treatment

	MCM	MCM/LRP6$^{fl/fl}$
Number	4	4
BW(g)	28.56±1.058	27.39±0.321
HW(mg)	127.9±3.318	120.0±3.658
HR (bmp)	517.8±8.892	495.0±10.98
LVAW;d (mm)	0.698±0.013	0.660±0.015
LVPW;d (mm)	0.655±0.025	0.650±0.021
LVID;d (mm)	3.983±0.096	3.770±0.141
EF (%)	73.34±1.478	73.79±1.976
FS (%)	42.09±1.268	42.84±2.057

Table S5. The functions involved in the differentiated proteins were analyzed by Ingenuity Pathway Analysis (IPA) Software.

Category	p-value
Cell-To-Cell Signaling and Interaction	1.12E-12-1.77E-03
Inflammatory Response	1.12E-12-1.56E-03
Cellular Function and Maintenance	1.19E-11-1.33E-03
Hematological System Development and Function	3.25E-11-1.56E-03
Metabolic Disease	8.26E-09-1.77E-03
Immune Cell Trafficking	1.06E-08-1.56E-03
Cellular Movement	1.5E-08-1.64E-03
Lipid Metabolism	2.72E-08-1.59E-03

Molecular Transport	2.72E-08-1.62E-03
Small Molecule Biochemistry	2.72E-08-1.77E-03
Organismal Injury and Abnormalities	5.22E-08-1.77E-03
Reproductive System Disease	6.04E-08-1.67E-03
Vitamin and Mineral Metabolism	6.53E-08-8.98E-04
Developmental Disorder	8.34E-08-1.29E-03
Hereditary Disorder	8.34E-08-1.77E-03
Neurological Disease	8.34E-08-1.5E-03
Dermatological Diseases and Conditions	1.21E-07-1.06E-03
Cell Death and Survival	1.38E-07-1.77E-03
Psychological Disorders	1.94E-07-1.27E-03
Connective Tissue Disorders	4.82E-07-9.35E-04
Ophthalmic Disease	4.82E-07-1.67E-03
Cardiovascular Disease	5.33E-07-1.77E-03
Embryonic Development	7.11E-07-1.29E-03
Protein Synthesis	7.98E-07-1.1E-03
Tissue Development	9.71E-07-1.56E-03
Organismal Functions	1.08E-06-1.02E-05
Gene Expression	1.23E-06-4.32E-05
Cellular Assembly and Organization	1.25E-06-1.74E-03
Hematological Disease	1.37E-06-1.77E-03
Skeletal and Muscular Disorders	1.76E-06-1.27E-03
Organ Morphology	2.83E-06-9.61E-04
Organismal Development	2.83E-06-1.29E-03
Renal and Urological Disease	2.83E-06-1.37E-03
Renal and Urological System Development and Function	2.83E-06-6.44E-04
Cancer	2.93E-06-1.74E-03
Cellular Growth and Proliferation	2.97E-06-1.72E-03
Nervous System Development and Function	3.3E-06-1.09E-03
Tissue Morphology	3.65E-06-1.29E-03
Organismal Survival	4.12E-06-7.4E-05
Infectious Diseases	4.77E-06-1.77E-03
Cardiovascular System Development and Function	5.76E-06-1.57E-03
Immunological Disease	6.03E-06-1.43E-03
Connective Tissue Development and Function	7.28E-06-1.37E-03
Inflammatory Disease	8.52E-06-1.06E-03
Endocrine System Disorders	1.28E-05-7.01E-04
DNA Replication, Recombination, and Repair	1.35E-05-1.36E-03
Cellular Development	1.62E-05-1.72E-03
Lymphoid Tissue Structure and Development	1.62E-05-3.56E-05
Cell Signaling	1.67E-05-1.02E-03
Carbohydrate Metabolism	1.76E-05-1.77E-03
Free Radical Scavenging	2.06E-05-1.65E-03
Organ Development	2.29E-05-5.34E-04

Skeletal and Muscular System Development and Function	2.29E-05-1.09E-03
Cell Morphology	6.15E-05-1.77E-03
Protein Degradation	6.16E-05-1.03E-04
Protein Trafficking	7.18E-05-5.72E-04
Gastrointestinal Disease	8.05E-05-1.56E-03
Hepatic System Disease	8.05E-05-1.56E-03
Tumor Morphology	8.84E-05-9.98E-04
Hair and Skin Development and Function	1.25E-04-1.77E-03
Cellular Compromise	1.34E-04-1.36E-03
Reproductive System Development and Function	1.34E-04-2.23E-04
Hypersensitivity Response	1.65E-04-1.65E-04
Digestive System Development and Function	2E-04-9.2E-04
Nutritional Disease	2E-04-7.91E-04
Post-Translational Modification	2.66E-04-1.37E-03
Cell-mediated Immune Response	5.11E-04-5.11E-04
Nucleic Acid Metabolism	5.17E-04-5.17E-04
Hepatic System Development and Function	6.07E-04-9.2E-04
Respiratory Disease	7.98E-04-1.5E-03
Behavior	1.02E-03-1.02E-03
Cell Cycle	1.05E-03-1.05E-03
Endocrine System Development and Function	1.62E-03-1.62E-03

Table S6. The pathways associated with differentiated proteins were analyzed by Ingenuity Pathway Analysis (IPA) Software.

Ingenuity Canonical Pathways	-log(p-value)	Ratio
LXR/RXR Activation	6.49	0.0579
FXR/RXR Activation	6.37	0.0556
PPARα/RXRα Activation	5.37	0.0393
eNOS Signaling	4.63	0.0387
Acute Phase Response Signaling	4.42	0.0355
ERK/MAPK Signaling	4.02	0.0302
Atherosclerosis Signaling	3.97	0.0394
Clathrin-mediated Endocytosis Signaling	3.09	0.0254
Aryl Hydrocarbon Receptor Signaling	2.74	0.0286
IL-12 Signaling and Production in Macrophages	2.68	0.0274
Caveolar-mediated Endocytosis Signaling	2.64	0.0423
Granzyme A Signaling	2.61	0.1
Protein Ubiquitination Pathway	2.59	0.0196
Aldosterone Signaling in Epithelial Cells	2.48	0.0241
Glucocorticoid Receptor Signaling	2.38	0.0174
Sertoli Cell-Sertoli Cell Junction Signaling	2.37	0.0225
Regulation of Actin-based Motility by Rho	2.33	0.033
Reelin Signaling in Neurons	2.32	0.0326

Death Receptor Signaling	2.32	0.0326
Sonic Hedgehog Signaling	2.26	0.0667
Production of Nitric Oxide and Reactive Oxygen Species in Macrophages	2.24	0.0207
Virus Entry via Endocytic Pathways	2.19	0.0294
Androgen Signaling	2.09	0.027
Nitric Oxide Signaling in the Cardiovascular System	2.07	0.0265
Netrin Signaling	2.04	0.0513
Neuroprotective Role of THOP1 in Alzheimer's Disease	2.02	0.05
Actin Cytoskeleton Signaling	1.99	0.0175
Triacylglycerol Degradation	1.92	0.0444
Ascorbate Recycling (Cytosolic)	1.83	0.25
Glutathione Redox Reactions II	1.83	0.25
Glycerol-3-phosphate Shuttle	1.83	0.25
Amyloid Processing	1.82	0.0392
Phototransduction Pathway	1.78	0.0377
Unfolded protein response	1.77	0.037
Eumelanin Biosynthesis	1.74	0.2
Hepatic Cholestasis	1.68	0.0189
Glycerol Degradation I	1.66	0.167
PXR/RXR Activation	1.62	0.0308
Gap Junction Signaling	1.61	0.0179
Axonal Guidance Signaling	1.6	0.0112
Germ Cell-Sertoli Cell Junction Signaling	1.58	0.0173
RhoGDI Signaling	1.58	0.0173
Agrin Interactions at Neuromuscular Junction	1.57	0.029
Granulocyte Adhesion and Diapedesis	1.55	0.0169
Calcium Signaling	1.55	0.0169
Melatonin Signaling	1.55	0.0282
GPCR-Mediated Integration of Enteroendocrine Signaling Exemplified by an L Cell	1.54	0.0278
BMP signaling pathway	1.49	0.0263

Table S7. The part of reported proteins or enzymes which interact with Drp1 were analyzed by Ingenuity Pathway Analysis (IPA) Software.

#NAME	Entrez Gene Name	Location	Family	Entrez Gene ID for Mouse
DNM1	dynamin 1	Cytoplasm	enzyme	13429
DNM1L	dynamin 1-like	Cytoplasm	enzyme	74006
Dynamin		Cytoplasm	group	

GSK3B	glycogen synthase kinase 3 beta	Nucleus	kinase	56637
MFF	mitochondrial fission factor	Cytoplasm	other	
Mff	mitochondrial fission factor	Cytoplasm	other	75734
MFN1	mitofusin 1	Cytoplasm	enzyme	67414
MFN2	mitofusin 2	Cytoplasm	enzyme	170731
MIEF1	mitochondrial elongation factor 1	Cytoplasm	other	239555
MIEF2	mitochondrial elongation factor 2	Cytoplasm	other	237781
MTOR	**mechanistic target of rapamycin (serine/threonine kinase)**	Nucleus	kinase	**56717**
MUL1	mitochondrial E3 ubiquitin protein ligase 1	Cytoplasm	enzyme	68350
MYH10	myosin, heavy chain 10, non-muscle	Cytoplasm	other	77579
MYH9	myosin, heavy chain 9, non-muscle	Cytoplasm	enzyme	17886
NTRK1	neurotrophic tyrosine kinase, receptor, type 1	Plasma Membrane	kinase	18211
NUFIP1	nuclear fragile X mental retardation protein interacting protein 1	Nucleus	other	27275
OMA1	OMA1 zinc metallopeptidase	Cytoplasm	peptidase	67013
OPA1	optic atrophy 1 (autosomal dominant)	Cytoplasm	enzyme	74143
OSM	oncostatin M	Extracellular Space	cytokine	18413
PARK2	parkin RBR E3 ubiquitin protein ligase	Cytoplasm	enzyme	50873
PEX11B	peroxisomal biogenesis factor 11 beta	Cytoplasm	other	18632
PEX14	peroxisomal biogenesis factor 14	Cytoplasm	transcription regulator	56273
PGAM5	PGAM family member 5, serine/threonine protein phosphatase, mitochondrial	Cytoplasm	enzyme	72542
PIM1	Pim-1 proto-oncogene, serine/threonine kinase	Cytoplasm	kinase	18712
PKP3	plakophilin 3	Plasma Membrane	other	56460
PSEN1	presenilin 1	Plasma Membrane	peptidase	19164
RAB32	RAB32, member RAS oncogene family	Cytoplasm	enzyme	67844
RRM2	ribonucleotide reductase M2	Nucleus	enzyme	20135
SCG3	secretogranin III	Extracellular Space	other	20255
SH3GL1	SH3-domain GRB2-like 1	Cytoplasm	other	20405
SIRT3	sirtuin 3	Cytoplasm	enzyme	64384
SLC1A2	solute carrier family 1 (glial high affinity glutamate transporter), member 2	Plasma Membrane	transporter	20511
SNCA	synuclein, alpha (non A4 component of amyloid precursor)	Cytoplasm	other	20617
SOX2	SRY (sex determining region Y)-box 2	Nucleus	transcription regulator	20674

TARDBP	TAR DNA binding protein	Nucleus	transcription regulator	230908
TP53	tumor protein p53	Nucleus	transcription regulator	22059
UBC	ubiquitin C	Cytoplasm	enzyme	22190
UBE2H	ubiquitin-conjugating enzyme E2H	Other	enzyme	22214
UBE2I	ubiquitin-conjugating enzyme E2I	Nucleus	enzyme	22196
Ubiquitin		Cytoplasm	group	
UNK	unkempt family zinc finger	Nucleus	transporter	217331
ZBTB24	zinc finger and BTB domain containing 24	Nucleus	other	268294

Supplementary figures and figure legends

Figure S1

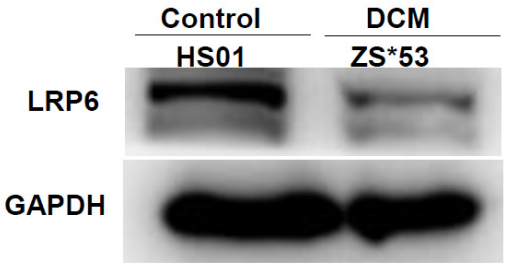

Figure S1. Western blot analysis of LRP6 expression in heart samples numbered HS01 (Control) and ZS13167553 (DCM).

Figure S2

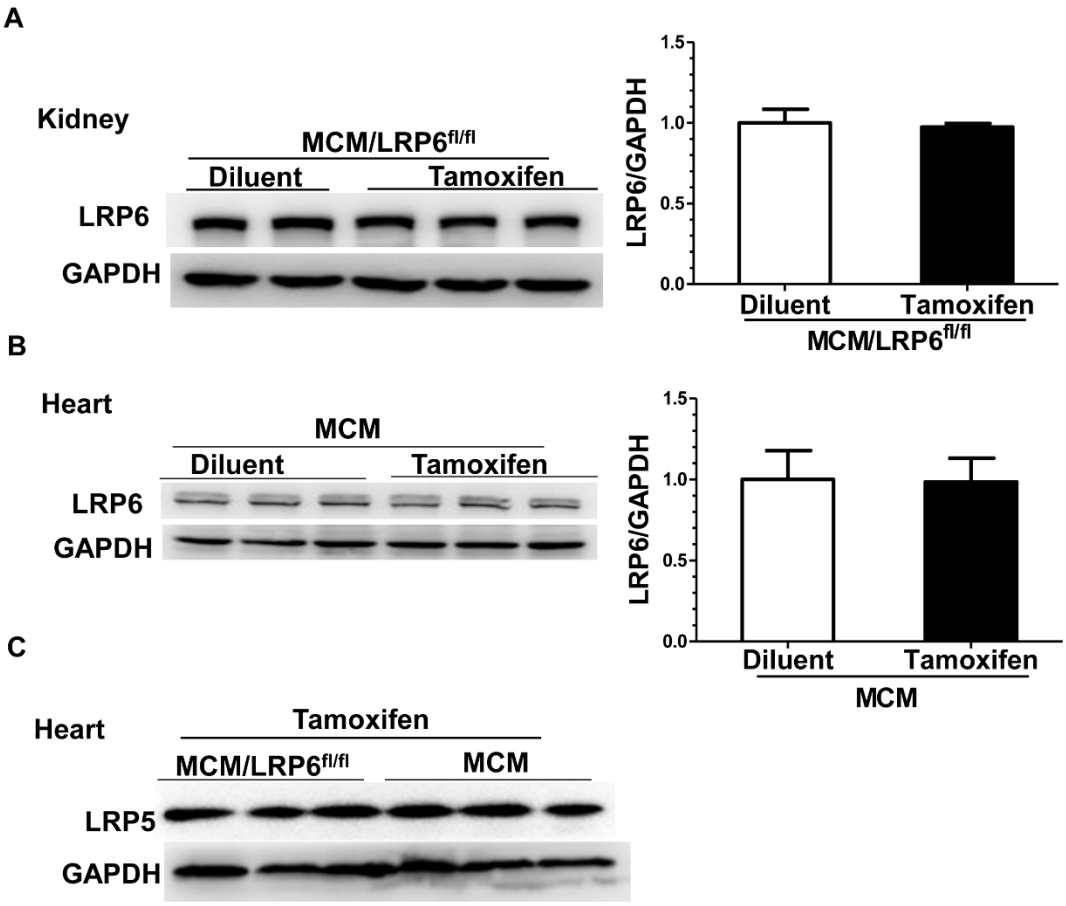

Figure S2. Analysis of LRP6 expression. (A) Western blot analysis of LRP6 expression in kidney tissue from MCM/LRP6$^{fl/fl}$ mice after three-day consecutive treatment with diluent (corn oil) or tamoxifen. (B) Western blot analysis of LRP6 expression in heart tissue from MCM mice after three-day consecutive treatment with diluent or tamoxifen. n=3/group. (C) Western blot analysis of LRP5 expression in heart tissue from MCM and MCM/LRP6$^{fl/fl}$ after three-day consecutive treatment with tamoxifen. n=3/group.

Figure S3

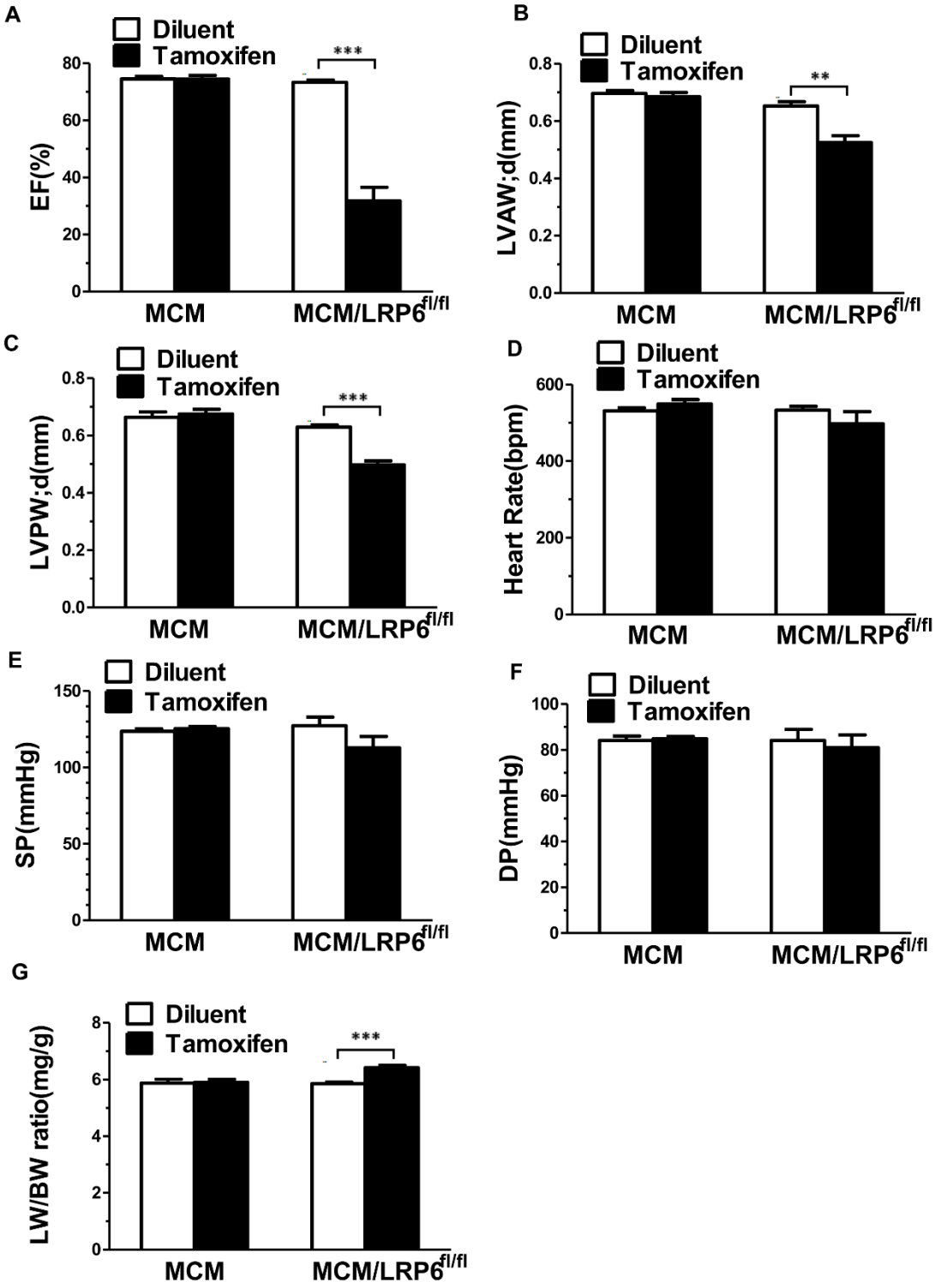

Figure S3. Echocardiographic and hemodynamic analysis. (A) Ejection fraction (EF). (B)Left ventricular diastolic anterior wall thickness (LVAW,d), (C)left ventricular diastolic posterior wall thickness (LVPW,d), (D) Heart rate (HR) (n=4-8/group). (E) Left ventricular systolic pressure (LVSP). (F) Left ventricular end diastolic pressure

(LVEDP). n=4-8/group. (G) Lung weight and body weight ratio (LW/BW) (n=6-12/group). MCM mice or MCM/LRP6$^{fl/fl}$ mice were treated three-day consecutive injection with diluent or tamoxifen. 2 days after the treatment, the mice were examined by echocardiography and hemodynamics analysis. ** p<0.01; *** p<0.001 *vs* diluent group.

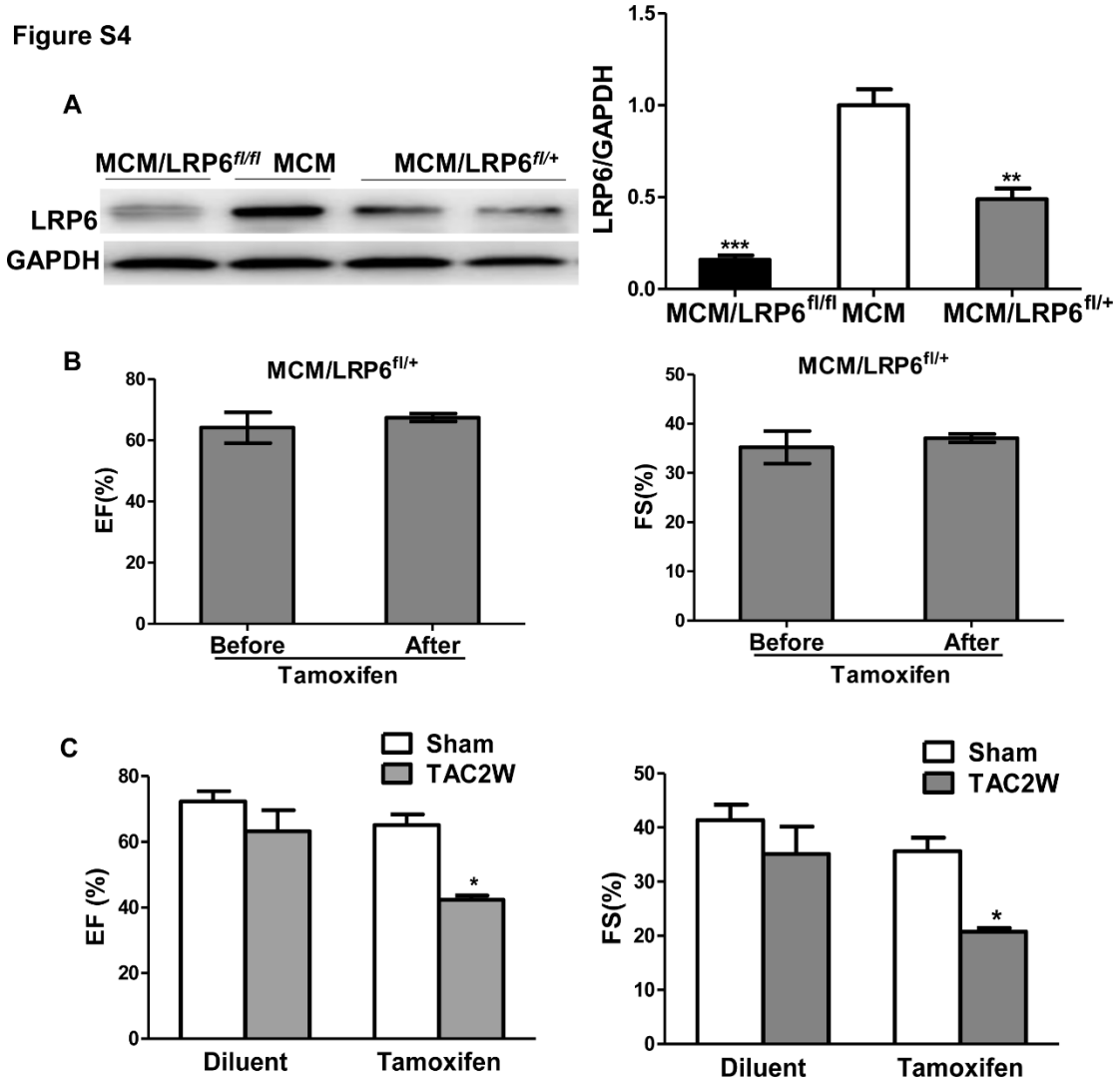

Figure S4. Echocardiography analysis of cardiac function in MCM/LRP6$^{fl/+}$. (a) Western blot analysis of LRP6 expression in heart tissue from MCM/LRP6$^{fl/+}$, MCM or MCM/LRP6$^{fl/fl}$ after three-day consecutive injection with tamoxifen. ** p<0.01,*** p<0.001 *vs* MCM group. n=3/group. (b) EF and FS were examined in MCM/LRP6$^{fl/fl}$ before or at day 2 after tamoxifen injection (n=3-6/group). (c) EF and FS were examined in tamoxifen-injected-MCM/LRP6$^{fl/+}$ or diluent-injected-ones at 2 weeks after TAC or sham operation. n=4-7/group. * p<0.05 vs sham group.

Figure S5

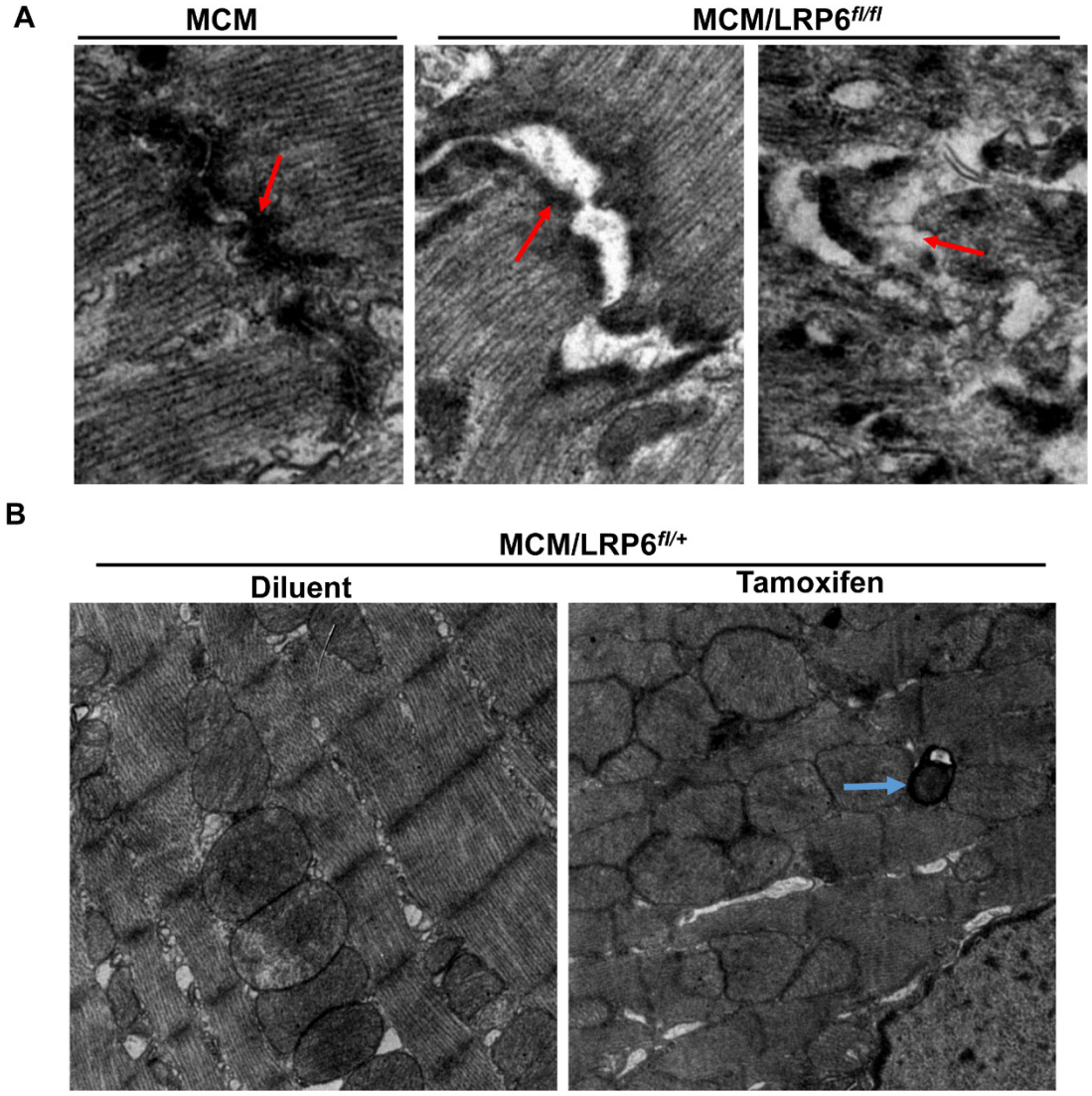

Figure S5. Representative electron microscope images of hearts from MCM/LRP6$^{fl/fl}$ and MCM mice at day 2 after 3-day consecutive injection with tamoxifen (A) and MCM/LRP6$^{fl/+}$ injected with tamoxifen or diluent (B). Architecture of Intercalated Disk (ID) was marked with red arrow. n=7-9/group. Mitochondrial targeting to autophagosome was marked with blue arrow. n=3/group.

Figure S6

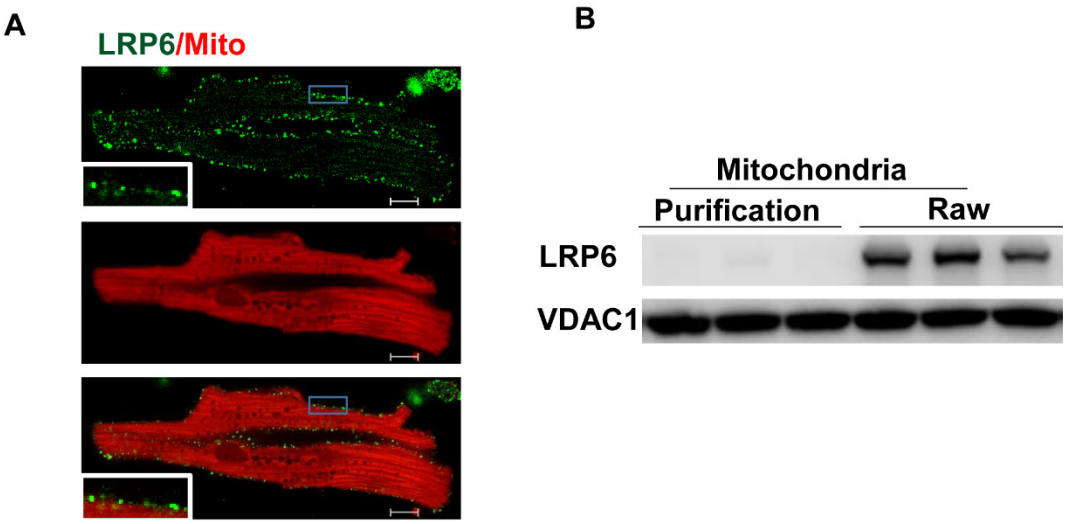

Figure S6. Analysis of LRP6 expression in cardiac mitochondria. (A) Immunostaining analysis of LRP6 expression in isolated cardiomyocyte from adult C57BL/6 mice. Green: LRP6; Red: mitochondria. Scale bar: 10μm. (B) Western blot analysis of LRP6 expression in raw and purified mitochondria in MCM/LRP6$^{fl/fl}$ without tamoxifen injection. n=3/group.

Figure S7

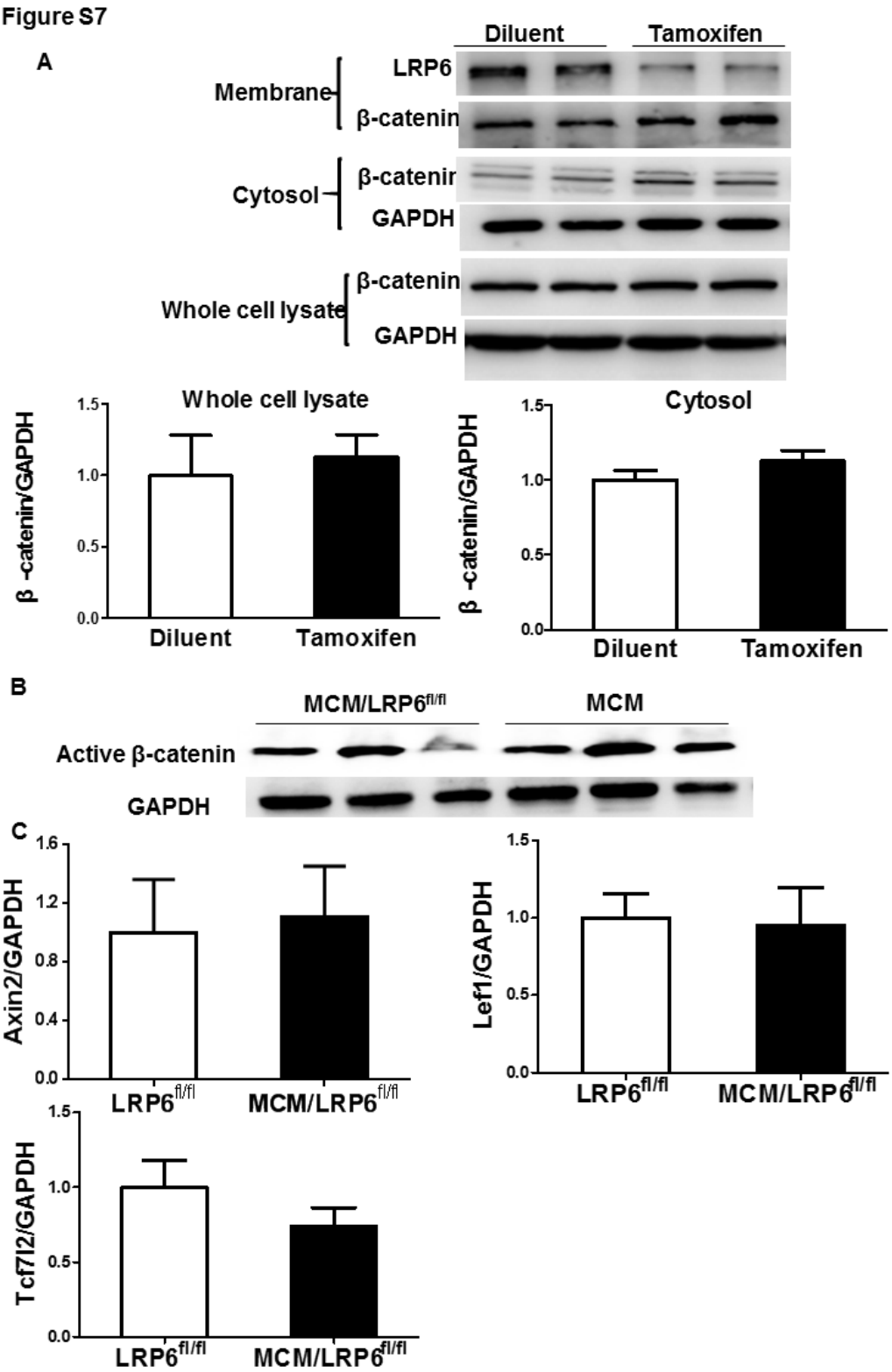

Figure S7. Analysis of wnt/β-catenin signaling. (A) Western analysis of β-catenin expression in membrane, cytosol and whole cell lysate from left ventricular tissue of MCM/LRP6 $^{fl/fl}$ at day 2 after diluent or tamoxifen treatments.(B) Western blot analysis of active β-catenin expression in left ventricular tissue from MCM or MCM/LRP6 $^{fl/fl}$

injected with tamoxifen. N=3/group. (C) Real-time PCR analysis of mRNA of β-catenin target genes (Axin2, Lef1 and Tcf7l2) in MCM/LRP6$^{fl/fl}$ or LRP6$^{fl/fl}$ injected with tamoxifen. n=3-4/group.

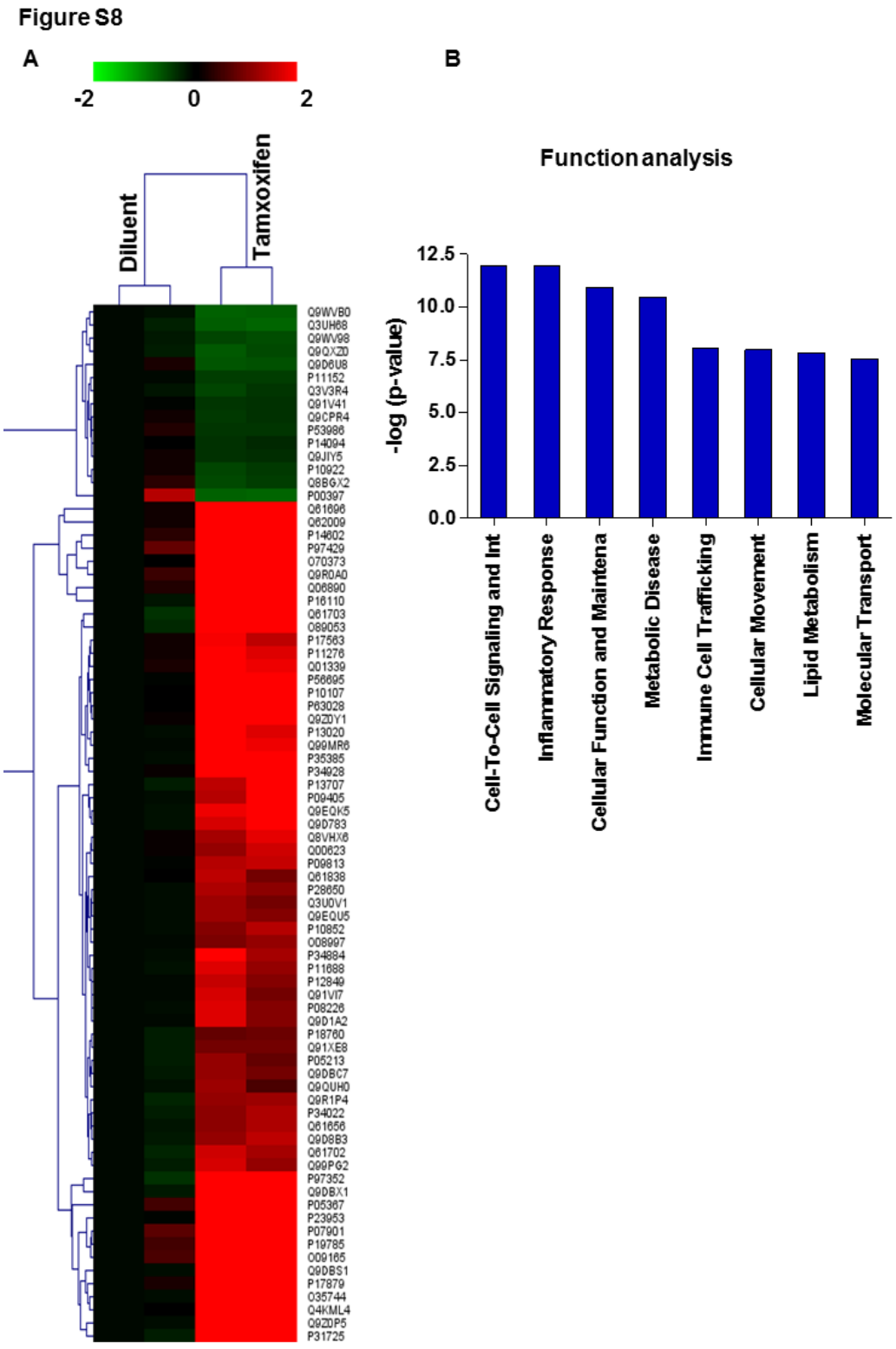

Figure S8. Proteomics analysis of heart tissue from MCM/LRP6$^{fl/fl}$ at day 1 after diluent

or tamoxifen treatments. (A) Identification of down-regulated (Green) (fold change <0.67) and up-regulated (Red) (fold change >1.2) cardiac proteins in tamoxifen-injected -MCM/LRP6$^{fl/fl}$ *vs* Diluent-injected-ones. (B) Top eight functions associated with differentiated proteins were analyzed by Ingenuity Pathway Analysis (IPA) Software.

Figure S9

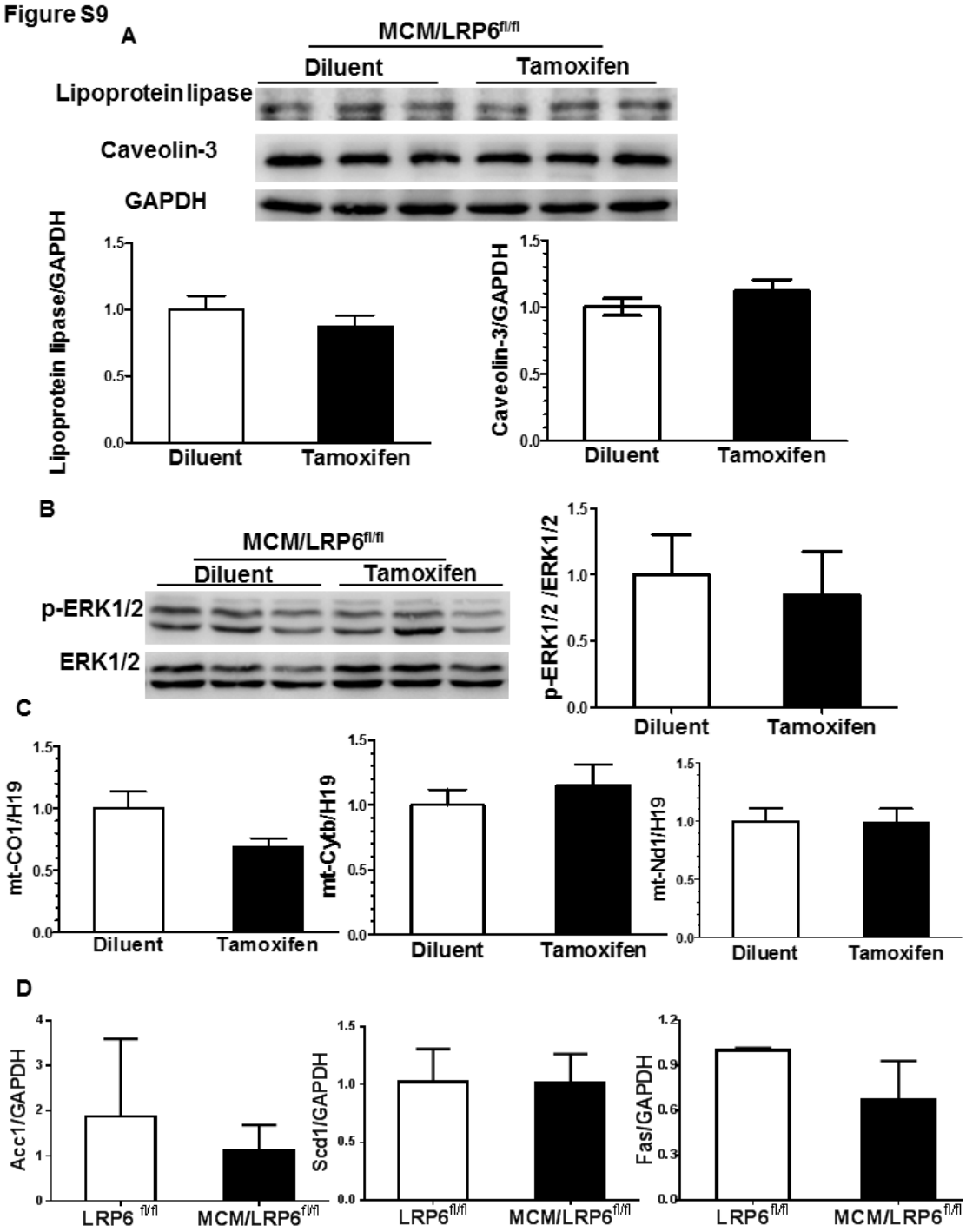

Figure S9. Identification of pathways or proteins indicated by proteomics analysis. (A) Western blot analysis of the expression of lipoprotein lipase and caveolin-3 in heart tissue from MCM/LRP6$^{fl/fl}$ at day 1 after three-day consecutive injection with diluent or tamoxifen. N=3/group. (B) Western blot analysis of p-ERK1/2 in heart tissue as the

same group in A. N=3/group. (C) qPCR analysis of relative content of *cytb,nd1* and *cox,* three mitochondrial gene targets, in heart homogenate from the mice as same group in B. *H19* genomic DNA target was used as an endogenous control. N=8/group. (D) qPCR analysis of relative content of *Acc1,Scd1 and Fas,* genes related to lipogenesis, in heart homogenate from MCM/LRP6$^{fl/fl}$ andLRP6$^{fl/fl}$ injected with tamoxifen. n=3-4/group.

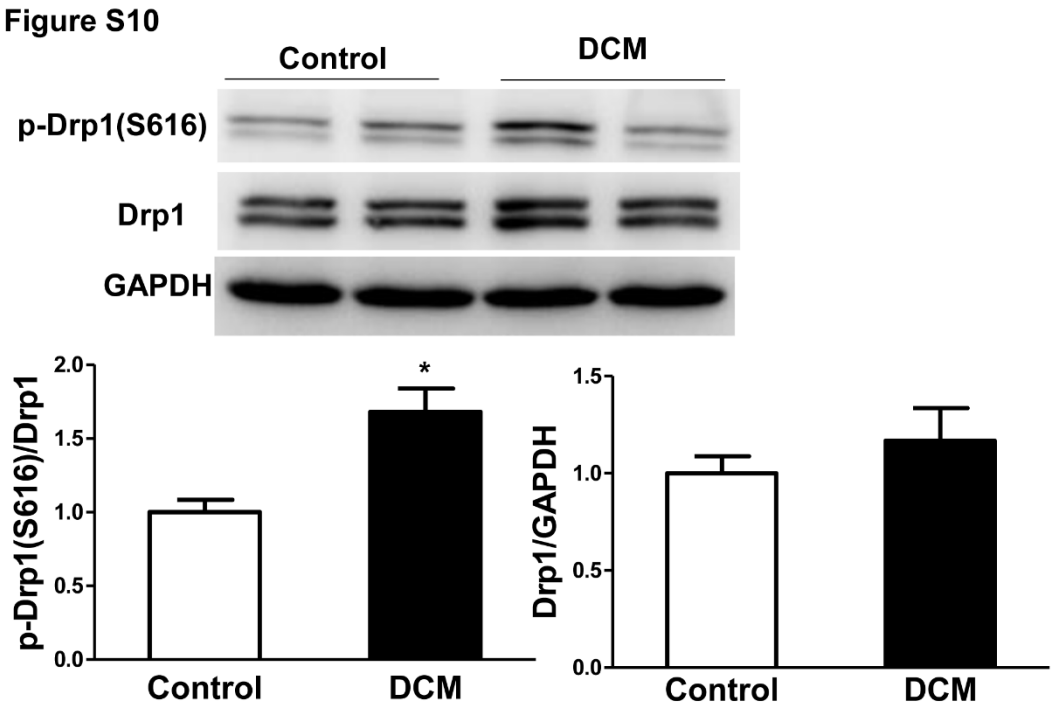

Figure S10. Western blot analysis of p-Drp1 (ser616) level. (A) p-Drp1 (ser616) and Drp1 level in control and DCM hearts. * $p<0.05$ vs. control group (n=3/group).

Figure S11

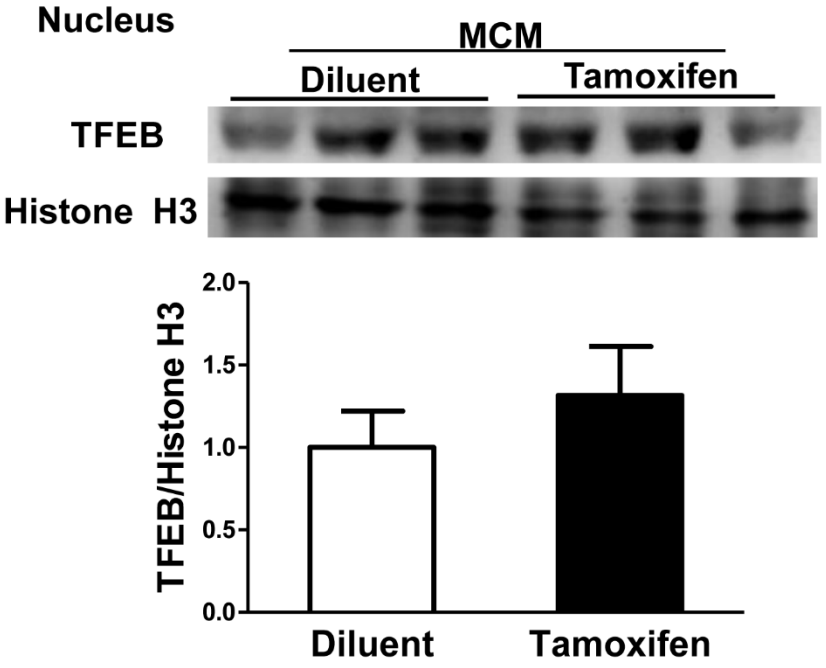

Figure S11. The nuclear TFEB expression was analyzed in heart tissue from MCM mice at day 1 after three-day consecutive treatment with diluent (corn oil) or tamoxifen. n=3/group.

Figure S12

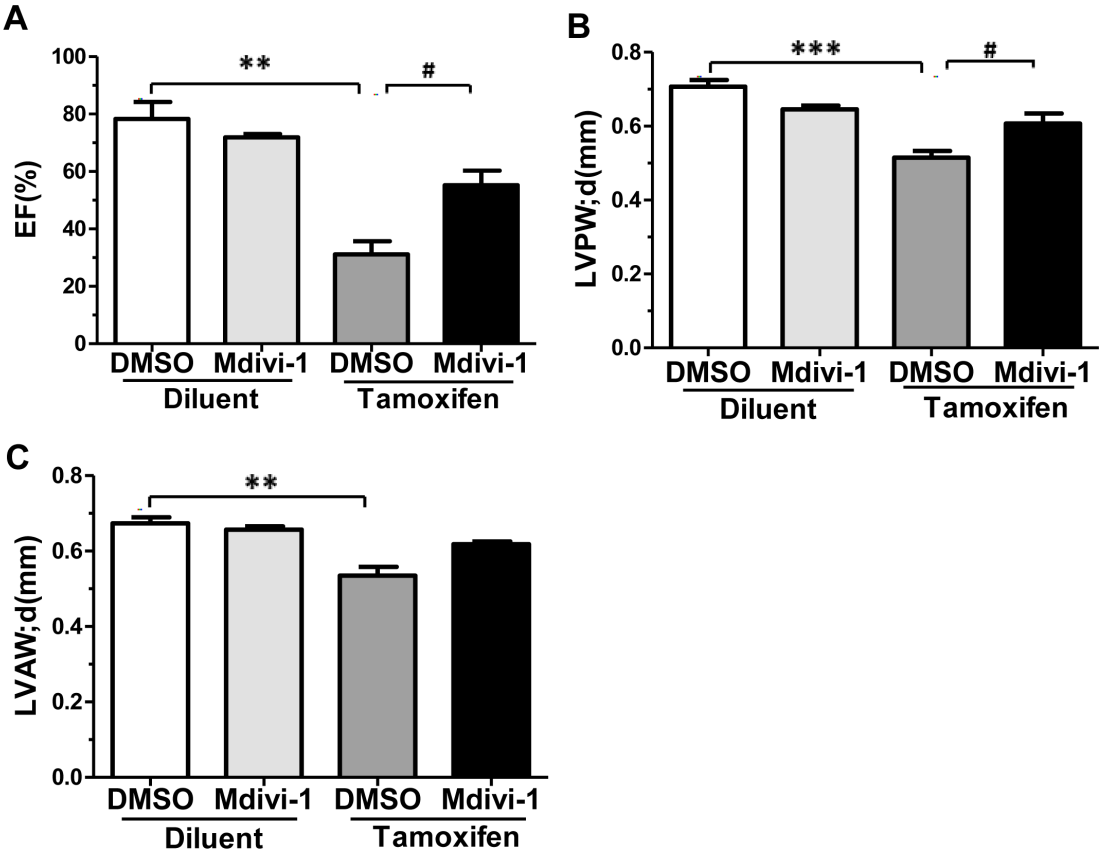

Figure S12. Echocardiographic and hemodynamic analysis. (A) EF. (B) LVPW;d. (C) LVAW;d. After three-day consecutive treatment with diluent or tamoxifen, MCM/LRP6$^{fl/fl}$ mice treated with DMSO or mdivi-1, immediately. ** $p<0.01$; *** $p<0.001$ *vs* DMSO+Diluent; $^{\#}p<0.05$ *vs* DMSO+Tamoxifen.

Reference

1. Gilar M, Olivova P, Daly AE, Gebler JC. Two-dimensional separation of peptides using RP-RP-HPLC system with different pH in first and second separation dimensions. J Sep Sci. 2005; 28: 1694-703.
2. Yang X, Dondeti V, Dezube R, Maynard DM, Geer LY, Epstein J, et al. DBParser: web-based software for shotgun proteomic data analyses. J Proteome Res. 2004; 3: 1002-8.
3. Peng J, Elias JE, Thoreen CC, Licklider LJ, Gygi SP. Evaluation of multidimensional chromatography coupled with tandem mass spectrometry (LC/LC-MS/MS) for large-scale protein analysis: the yeast proteome. J Proteome Res. 2003; 2: 43-50.
4. Zhang J, Li X, Mueller M, Wang Y, Zong C, Deng N, et al. Systematic characterization of the murine mitochondrial proteome using functionally validated cardiac mitochondria. Proteomics. 2008; 8: 1564-75.
5. Wang X, Ye Y, Gong H, Wu J, Yuan J, Wang S, et al. The effects of different angiotensin II type 1 receptor blockers on the regulation of the ACE-AngII-AT1 and ACE2-Ang(1-7)-Mas axes

in pressure overload-induced cardiac remodeling in male mice. J Mol Cell Cardiol. 2016; 97: 180-90.
6. Zhu XJ, Shi Y, Peng J, Guo CS, Shan NN, Qin P, et al. The effects of BAFF and BAFF-R-Fc fusion protein in immune thrombocytopenia. Blood. 2009; 114: 5362-7.
7. Wang G, Liem DA, Vondriska TM, Honda HM, Korge P, Pantaleon DM, et al. Nitric oxide donors protect murine myocardium against infarction via modulation of mitochondrial permeability transition. Am J Physiol-HEART C. 2005; 288: H1290-5.
8. Mei Z, Wang X, Liu W, Gong J, Gao X, Zhang T, et al. Mitochondrial adaptations during myocardial hypertrophy induced by abdominal aortic constriction. Cardiovasc Pathol. 2014; 23: 283-8.
9. Shirakabe A, Zhai P, Ikeda Y, Saito T, Maejima Y, Hsu CP, et al. Drp1-Dependent Mitochondrial Autophagy Plays a Protective Role Against Pressure Overload-Induced Mitochondrial Dysfunction and Heart Failure. Circulation. 2016; 133: 1249-63.
10. Gao W, Liu H, Yuan J, Wu C, Huang D, Ma Y, et al. Exosomes derived from mature dendritic cells increase endothelial inflammation and atherosclerosis via membrane TNF-alpha mediated NF-kappaB pathway. J Cell Mol Med. 2016; 20(12):2318-2327.
11. An Y, Xu W, Li H, Lei H, Zhang L, Hao F, et al. High-fat diet induces dynamic metabolic alterations in multiple biological matrices of rats. J Proteome Res. 2013; 12: 3755-68.